

# Field-Effect Modulation of Seebeck Coefficient in Single PbSe Nanowires

Wenjie Liang,<sup>†,||</sup> Allon I. Hochbaum,<sup>†</sup> Melissa Fardy,<sup>†</sup> Oded Rabin,<sup>†,§</sup>  
Minjuan Zhang,<sup>‡</sup> and Peidong Yang<sup>\*,†</sup>

Department of Chemistry, University of California at Berkeley, Berkeley, California 94720, and Materials Research Department, Toyota Technical Center, Toyota Motor Engineering & Manufacturing North America (TEMA) Inc., 1555 Woodridge Avenue, Ann Arbor, Michigan 48105

Received February 5, 2009

## ABSTRACT

In this Letter, we present a novel strategy to control the thermoelectric properties of individual PbSe nanowires. Using a field-effect gated device, we were able to tune the Seebeck coefficient of single PbSe nanowires from 64 to 193  $\mu\text{V}\cdot\text{K}^{-1}$ . This direct electrical field control of  $\sigma$  and  $S$  suggests a powerful strategy for optimizing  $ZT$  in thermoelectric devices. These results represent the first demonstration of field-effect modulation of the thermoelectric figure of merit in a single semiconductor nanowire. This novel strategy for thermoelectric property modulation could prove especially important in optimizing the thermoelectric properties of semiconductors where reproducible doping is difficult to achieve.

Solid-state thermoelectric modules<sup>1</sup> have garnered increased attention due to their prospective application as power cogenerators, harvesting the vast amount of waste heat produced by combustion-based power generators.<sup>2</sup> The efficiency of energy conversion in such materials depends on the dimensionless thermoelectric figure of merit,  $ZT = \sigma S^2 T / \kappa$ , where  $\sigma$  is the electrical conductivity,  $S$  is the thermoelectric power (also called the Seebeck coefficient),  $\kappa$  is the thermal conductivity, and  $T$  is the absolute temperature.<sup>3</sup> Although  $\sigma$ ,  $S$ , and  $\kappa$  are interdependent in bulk materials such that a  $ZT$  greater than 1 is difficult to achieve, experimental and theoretical studies of nanostructured materials suggest that these parameters could be modified independently in low-dimensional systems.<sup>4–10</sup> Here we present a novel strategy to control the thermoelectric properties of individual PbSe nanowires. Using a field-effect gated device, we were able to tune the Seebeck coefficient of single PbSe nanowires from 64 to 193  $\mu\text{V}\cdot\text{K}^{-1}$ . This direct electrical field control of  $\sigma$  and  $S$  suggests a powerful strategy for optimizing  $ZT$  in thermoelectric devices.

Lead chalcogenides are promising thermoelectric materials that possess reasonably high thermoelectric conversion efficiencies. A  $ZT$  up to 2 was realized in PbSeTe/PbTe quantum dot superlattices,<sup>6</sup> and theoretical studies by Dresselhaus and co-workers have suggested that this number can be further increased in electronically confined nanowire structures.<sup>4,5</sup> Recent work, moreover, has demonstrated large decreases in the thermal conductivity of nanowire systems.<sup>8</sup> The PbSe nanowires discussed here were synthesized via a solution-phase method described previously by Murray and co-workers.<sup>11</sup> The nanowires had diameters around 80 nm with lengths up to tens of micrometers. Transmission electron microscopy (TEM) images (Figure 1a) of the as-made nanowires show that these structures have extremely rough surfaces, probably as a consequence of growth via the oriented nanoparticle attachment and overgrowth mechanism. Despite their rough surfaces, the nanowires are single crystalline, as shown by the high-resolution TEM (HRTEM) images (Figure 1a, inset).

The thermoelectric properties of individual PbSe nanowires were measured using the circuit shown in Figure 2a. The circuit consists of a heater for establishing a temperature gradient and four electrical probes for measuring the conductivity and thermal voltage across the nanowire. The two inner electrical probes were each attached to four leads, allowing them to function simultaneously as resistive thermometers. The thermoelectric properties of the PbSe nanowires could be directly modulated during measurement by applying a gate voltage to the underlying silicon substrate,

<sup>†</sup> Department of Chemistry, University of California at Berkeley.

<sup>‡</sup> Toyota Technical Center, Toyota Motor Engineering & Manufacturing North America (TEMA) Inc.

<sup>§</sup> Current address: Department of Materials Science and Engineering and the Institute for Research in Electronics and Applied Physics, University of Maryland, College Park, MD 20742.

<sup>||</sup> Current address: Institute of Physics, Academy of Science, Haidian, Beijing, 100080, China.

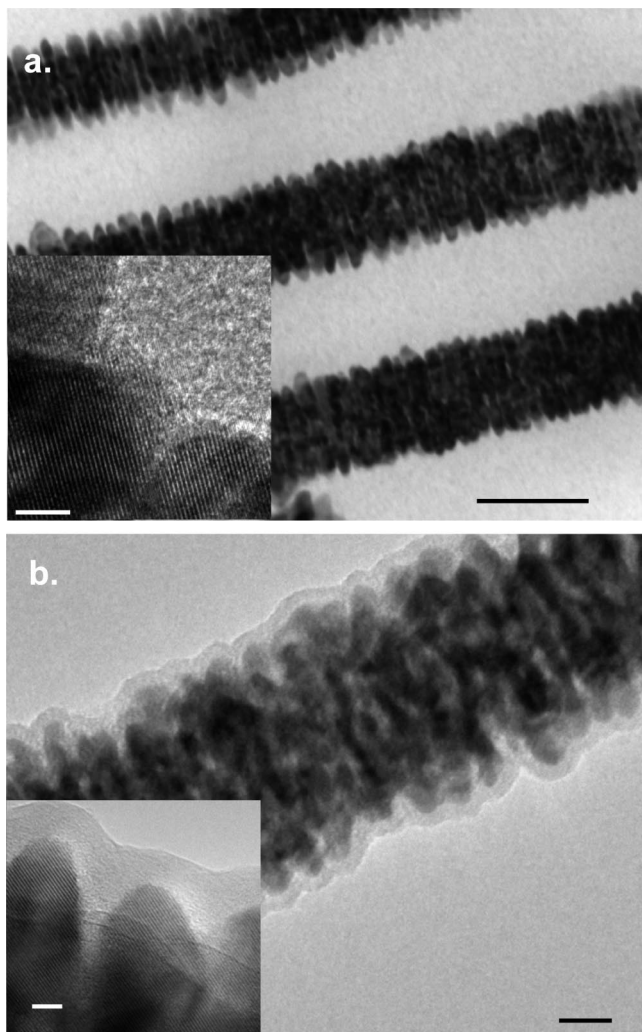


**Figure 1.** TEM images of PbSe nanowires: (a) as-synthesized PbSe nanowires; (b) PbSe nanowire coated with ALD alumina. Insets are HRTEM images of the corresponding nanowires. Scale bars for (a), (b), (a) inset, and (b) inset are 100, 20, 4, and 3nm, respectively.

similar to the carbon nanotube devices described in refs 12 and 13.

Although PbSe nanowires are relatively flexible at the size scale used in this study, they remain fragile and are very sensitive to processing steps and conditions such as thermal shock, mechanical stress, and oxidation. Consequently, great care was taken in every step of device fabrication. The as-synthesized nanowires were first dispersed in chloroform and cast by spin-coating onto a silicon substrate coated with a 600 nm SiN<sub>x</sub> film. Immediately upon evaporation of the solvent, the substrate was coated with I-line photoresist. Standard photolithographic processing was used to pattern the electrodes in Figure 2a. 1/150/35 nm Ti/Pd/Au metal films were then deposited by electron-beam evaporation. The evaporation step was divided into 5 min segments, between which the chip was allowed to cool down for 5 min to prevent overheating. Finally, the substrate was soaked in acetone for 30–60 min to dissolve the photoresist and lift off the metal film.

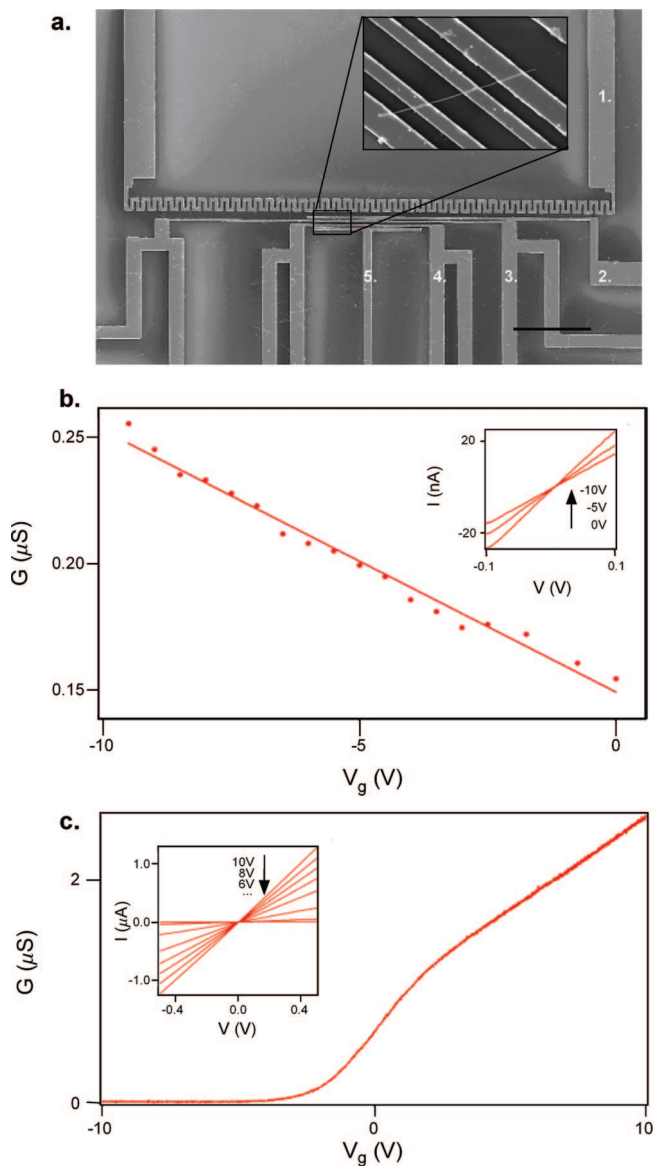


**Figure 2.** Electrical measurements of typical as-synthesized and Al<sub>2</sub>O<sub>3</sub> coated single PbSe nanowires. (a) Scanning electron microscopy image of the circuit used for electrical and thermoelectric power measurements of single PbSe nanowires. Electrode 1 is a heating line, and 2, 3, 4, and 5 are for four-point probe resistance measurements. Electrodes 3 and 4 are used as electrodes and resistive thermometers for the thermoelectric power measurement. PbSe nanowires were dispersed on a Si substrate coated with a 600 nm SiN<sub>x</sub> dielectric layer. Ti/Pd/Au electrodes were defined by photolithography and electron-beam evaporated on top of the dispersed nanowires. Inset shows a PbSe nanowire bridging electrodes 2–5. Scale bar is 50 μm. (b) Conductance of a as-synthesized single PbSe nanowire as a function of gate voltage ( $V_g$ ). Inset:  $I$ – $V$  behavior of the same PbSe nanowire taken at  $V_g = -10, -5, \text{ and } 0$  V. (c) Conductance of a single PbSe nanowire coated with Al<sub>2</sub>O<sub>3</sub> as a function of  $V_g$ . Inset:  $I$ – $V$  behavior of the same coated nanowire at  $V_g = 10, 8, 6, 4, 2, 0, \text{ and } -2$  V.

Due to the air sensitivity and chemical instability of the PbSe nanowires,<sup>11</sup> we have intentionally passivated the nanowire surface with a thin Al<sub>2</sub>O<sub>3</sub> film. After device fabrication the nanowires were first annealed under 700 mTorr of N<sub>2</sub> at 200 °C for up to 4 h. Atomic layer deposition

(ALD) methods were then used to deposit the Al<sub>2</sub>O<sub>3</sub> at 50 °C following procedures previously reported in ref 14. Figure 1b and inset show TEM and HRTEM images, respectively, of PbSe nanowires coated with ALD-deposited Al<sub>2</sub>O<sub>3</sub>. This procedure readily produced a conformal ~6 nm coating of Al<sub>2</sub>O<sub>3</sub> without altering the morphology, microstructure, or crystalline nature of the nanowires.

The low-temperature ALD method used to coat the PbSe nanowire devices with Al<sub>2</sub>O<sub>3</sub> effectively stabilized the air-sensitive PbSe nanowires. All previous electrical studies on PbSe nanostructures had to be performed under either inert atmosphere<sup>9,11,15</sup> or vacuum.<sup>16</sup> By using the Al<sub>2</sub>O<sub>3</sub> coating, we found our individual PbSe nanowire devices could be tested in ambient conditions without noticeable change for more than half a year. This strategy provides a practical route for stabilizing lead chalcogenide nanostructures, allowing them to be used in a broader range of applications.

Parts b and c of Figure 2 show typical electrical transport behavior of a single PbSe nanowire field-effect transistor before and after coating by ALD Al<sub>2</sub>O<sub>3</sub>. As shown in the insets, the current versus applied voltage ( $I - V$ ) plots at different gate voltages ( $V_g$ ) were all linear, indicating that Ohmic contacts were formed between the metal and nanowire in both cases. Typical values for the four-point resistance of individual nanowires were on the order of several hundred k $\Omega$ s and showed minimal (<0.5%) contact resistance. Single PbSe nanowires were able to conduct currents up to 10  $\mu$ A without failure, corresponding to a breakdown current density of approximately  $5 \times 10^5$  A $\cdot$ cm<sup>-2</sup>. These values, along with the TEM observations, indicate that these devices comprise high-quality, single crystalline nanowires with Ohmic contacts.

One significant difference in the electrical transport behavior before and after Al<sub>2</sub>O<sub>3</sub> coating is the sign of the charge carriers responsible for conduction in the nanowires. As shown in part b (and c) of Figure 2 the conductance of single nanowire transistors decreased (increased) with increasing  $V_g$  before (after) Al<sub>2</sub>O<sub>3</sub> deposition. These opposite trends indicate a switch in the polarity of free charge carriers due to the Al<sub>2</sub>O<sub>3</sub> coating; that is, PbSe nanowires were p-type before and n-type after coating. Considering the narrow band gap (280 meV)<sup>17</sup> and high reactivity of PbSe, changes in the electron density at the surface, either due to adsorbed species or chemical reactions, could readily affect the carrier density or polarity within the nanowire. For example, it was previously observed that treatment of PbSe nanoparticle films with hydrazine also changed the polarity of the majority charge carriers from p- to n-type.<sup>9,15</sup> Our ALD process could result in a positively surface-charged Al<sub>2</sub>O<sub>3</sub> film,<sup>18</sup> and we tentatively attribute the change in carrier type to the effective gating by the positively charged Al<sub>2</sub>O<sub>3</sub> layer.

The mobility of the charge carriers in the nanowires,  $\mu$ , can be extracted from their transconductance ( $dG/dV_g$ ) and geometric factors derived from modeling the nanowire field-effect transistor using a cylinder-plane capacitor model<sup>19,20</sup>

$$\mu = dG/dV_g \ln(2h/r)L/(2\pi\epsilon_0\epsilon)$$

where  $h$  is SiN<sub>x</sub> thickness,  $r$  and  $L$  are the nanowire radius

and length, and  $\epsilon_0$  is the vacuum permittivity and  $\epsilon$  is the SiN<sub>x</sub> relative dielectric constant. For two of the n-type PbSe nanowire devices, the drift mobilities were calculated to be 76 (Figure 2c) and 180 cm<sup>2</sup> $\cdot$ V<sup>-1</sup> $\cdot$ s<sup>-1</sup>. The charge carrier concentration was measured as  $1.8 \times 10^{18}$  cm<sup>-3</sup>. The as-synthesized p-type nanowires, on the other hand, exhibited much lower mobilities of about 3 cm<sup>2</sup> $\cdot$ V<sup>-1</sup> $\cdot$ s<sup>-1</sup>. The data in Figure 2b yields a mobility of 2.7 cm<sup>2</sup> $\cdot$ V<sup>-1</sup> $\cdot$ s<sup>-1</sup> and a carrier concentration of  $6 \times 10^{18}$  cm<sup>-3</sup>. A possible cause of the enhancement of mobility in Al<sub>2</sub>O<sub>3</sub>-coated samples could be the passivation of both surface defects and charge trap states by the high quality ALD Al<sub>2</sub>O<sub>3</sub> film. Although the highest mobility value measured is still an order of magnitude lower than observed values of the Hall mobility in bulk PbSe,<sup>21</sup> it is by far the largest mobility reported for lead chalcogenide nanostructures.<sup>15</sup> Further improvements in sample preparation and processing could augment these values. Additionally, we note that the model used to calculate the drift mobility from the transconductance provides only a lower bound of the actual value.<sup>20</sup> Overall, atomic layer deposition of alumina resulted in air-stable PbSe nanowire devices with inversion of charge polarity and enhanced carrier mobility. Field-effect gating of such PbSe nanowire devices readily changed their conductance by 2 orders of magnitude (Figure 2c).

To measure the thermoelectric power (Seebeck coefficient) of individual Al<sub>2</sub>O<sub>3</sub>-coated nanowires, a current was passed through the heater shown in Figure 2a (electrode 1), creating a thermal gradient across the nanowire bridging the electrodes. The voltage measured across the two inner electrodes (3 and 4 in Figure 2a) in the temperature gradient is the thermal voltage ( $V_{\text{therm}}$ ), from which the thermoelectric power,  $S$ , is calculated as  $S = V_{\text{therm}}/\Delta T$ . As shown in Figure 3a the measured  $V_{\text{therm}}$  values were plotted as a function of heating current,  $I_{\text{heat}}$ , applied to the heater. The parabolas correspond to  $V_{\text{therm}}$  measurements from the same nanowire under different applied  $V_g$ . The sign convention is such that negative  $V_{\text{therm}}$  values are measured for n-type samples due to the negative polarity of the majority charge carriers that transport heat, i.e.,  $V_{\text{therm}} < 0$  when electrode 3 has a higher voltage potential than electrode 4, as labeled in Figure 2a.

The negative values of  $V_{\text{therm}}$  are consistent with the charge carrier type determined by the transconductance measurements in Figure 2c. The temperature of the heater is proportional to the heating power and thus proportional to  $I_{\text{heat}}^2$ .  $V_{\text{therm}}$  as a function of  $I_{\text{heat}}$  was recorded in Figure 3a for different gate voltages (and hence different conductivities). The  $\Delta T$  along the nanowire was measured between the same two electrodes used to obtain  $V_{\text{therm}}$  and was calculated using a calibration of the metal line four-point resistance at fixed global temperatures. These data were then used to calculate the Seebeck coefficient of the nanowire.

Significantly, we observed clear modulation of the Seebeck coefficient in these PbSe nanowires by field-effect gating. This is, to the best of our knowledge, the first time such field-effect modulation of Seebeck coefficient is demonstrated at the single semiconductor nanowire level. The observed absolute value for thermoelectric power,  $S_{\text{abs}}$ , was measured as a function of the gate voltage (and hence PbSe nanowire



$$S = \frac{k_B}{e} \left( \frac{E_F - E_c}{k_B T} + A \right) \quad (2)$$

where  $A$  represents a scattering factor of the semiconductor.<sup>22,24</sup>

Varying  $V_g$  changes the electrical conductivity effectively by modulating the electron density in the conduction band and, hence,  $E_F$  of the nanowire. Using the general expression of  $E_F$  and electron density, eq 2 can be simplified to

$$S = C_1 (\ln N_c - \ln n + A) \quad (3)$$

where  $C_1$  is a fitting parameter,  $n$  is the carrier concentration, and  $N_c$  is the temperature-dependent effective density of states of the conduction band. Changes in the thermoelectric power via  $E_F$  modulation (and hence conductivity), as shown in Figure 3b, closely follow this relation in eq 3. Using the measured electron mobility of  $76 \text{ cm}^2 \text{ V}^{-1} \text{ s}^{-1}$  and assuming an effective mass ( $m_e^*$ ) of  $\sim 0.05 m_0$ ,<sup>17</sup>  $A$  is estimated to be 1.5. This result is consistent with the value of  $A$  in bulk PbSe,<sup>21,22</sup> suggesting that electron transport in the nanowire does not differ significantly from that in a classical system.

We have also measured the thermal conductivity of individual PbSe nanowires using suspended microfabricated membranes, as described in previous studies.<sup>8,25–27</sup> The thermal conductivity of a single PbSe nanowire was measured to be about  $0.8 \text{ W} \cdot \text{m}^{-1} \cdot \text{K}^{-1}$ , which is a 2-fold decrease from that of bulk PbSe at room temperature.<sup>28,29</sup> This reduction in thermal conductivity is likely the result of higher rates of phonon scattering at the nanowire surface. The surface roughness<sup>8</sup> may also play a role by scattering the intermediate and long wavelength phonon modes.

By combination of the results from the individual nanowire thermoelectric measurements, an estimation can be made for the figure of merit for single PbSe nanowires. Figure 3b also plots  $ZT$  as a function of electrical conductivity. It was found that there is a maximum in  $ZT$ , which occurs around  $16 (\Omega \cdot \text{cm})^{-1}$ . Room temperature  $ZT$  can be effectively tuned from 0.004 to 0.006, corresponding to changes in  $S$  by a factor of 3 and  $\sigma$  by 1 order of magnitude. More importantly, a net increase of the figure of merit by 50% is achieved through this simple field-effect gating strategy. These results represent the first demonstration of field-effect modulation of the thermoelectric figure of merit in a single semiconductor nanowire. This novel strategy for thermoelectric property modulation could prove especially important in optimizing the thermoelectric properties of semiconductors where reproducible doping is difficult to achieve.

The low figure of merit reported here is clearly the result of a drop in electron mobility from bulk values.<sup>29</sup> Such a reduction may be expected in quasi-one-dimensional materials since the surface-to-volume ratio increases considerably. Optimizing the surface passivation by improved synthetic techniques or surface treatments will undoubtedly improve the transport properties of PbSe nanowires and may yield lead chalcogenide nanowires with superior thermoelectric performance.

**Acknowledgment.** We thank Dr. Yue Wu and Renkun Chen for helpful discussions and Ruoxue Yan for assistance

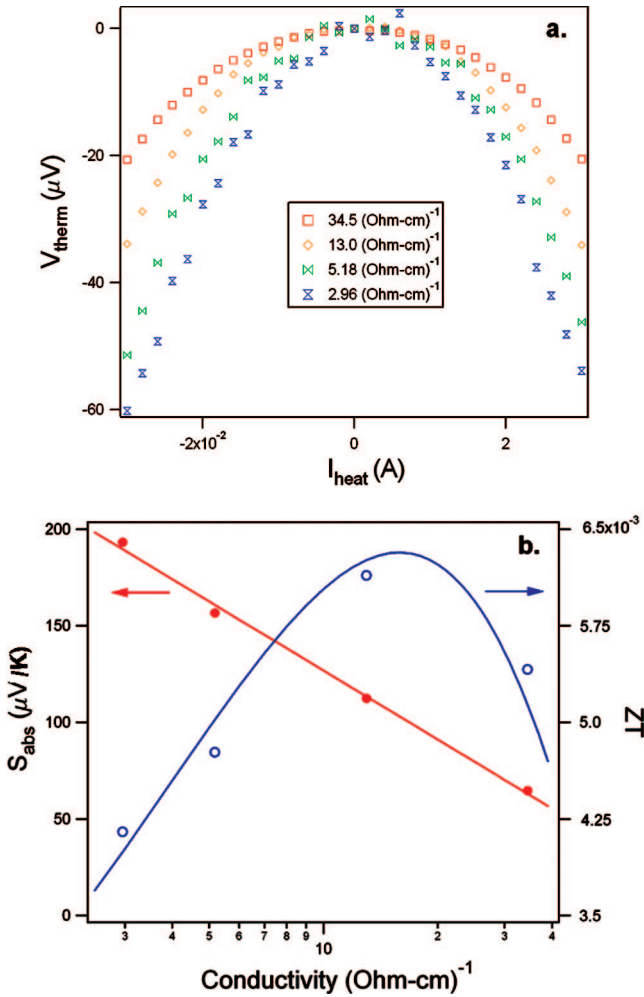


**Figure 3.** Thermoelectric power and figure-of-merit of an individual  $\text{Al}_2\text{O}_3$ -coated PbSe nanowire taken at different gate voltages. (a) Thermal voltages of an  $\text{Al}_2\text{O}_3$ -coated PbSe nanowire as a function of heater current taken at various values of nanowire conductivity, as defined by the applied gate voltage. (b) Seebeck coefficient (red) and the estimated room temperature  $ZT$  (blue) as a function of the nanowire conductivity, defined by the applied gate voltage.

conductivity) and the magnitude of  $S_{\text{abs}}$  was observed to decrease with increasing sample conductivity, as shown in Figure 3b. Room temperature values for  $S_{\text{abs}}$  ranged from 64 to  $193 \mu\text{V} \cdot \text{K}^{-1}$  under high to low  $V_g$ , respectively. This represents direct field-effect modulation of the Seebeck coefficient by a factor of 3. The general expression for  $S$  is<sup>22,23</sup>

$$S = \frac{k_B}{e} \int \frac{E_F - E}{k_B T} \frac{\sigma(E)}{\sigma} dE \quad (1)$$

where  $k_B$  is the Boltzmann constant,  $e$  is the electron charge,  $E_F$  is the Fermi energy of the material,  $\sigma(E)$  is the electrical conductivity at a given electron energy,  $E$ , and  $\sigma$  is the total conductivity. Assuming that only electrons contribute to the thermoelectric power and that  $E_F$  lies near the conduction band edge ( $E_c$ ), the above equation can be written as

with ALD film preparation. We also thank the National Center for Electron Microscopy and the UC Berkeley Microlab for the use of their facilities.

**Supporting Information Available:** A description of experimental methods. This material is available free of charge via the Internet at <http://pubs.acs.org>.

## References

- (1) Dresselhaus, M.; Chen, G.; Tang, M. Y.; Yang, R. G.; Lee, H.; Wang, D. Z.; Ren, Z. F.; Fleurial, J.-P.; Gogna, P. New directions for low-dimensional thermoelectric materials. *Adv. Mater.* **2007**, *19*, 1043–1053.
- (2) Majumdar, A. Thermoelectricity in semiconductor nanostructures. *Science* **2004**, *303*, 777–778.
- (3) Goldsmid, H. Thermoelectric refrigeration; Plenum Press: New York, 1964.
- (4) Hicks, L.; Dresselhaus, M. Effect of quantum-well structures on the thermoelectric figure of merit. *Phys. Rev. B* **1993**, *47*, 12727–12731.
- (5) Hicks, L. D.; Dresselhaus, M. S. Thermoelectric figure of merit of a one-dimensional conductor. *Phys. Rev. B* **1993**, *47*, 16631–16634.
- (6) Harman, T. C.; Taylor, P. J.; Walsh, M. P.; LaForge, B. E. Quantum dot superlattice thermoelectric materials and devices. *Science* **2004**, *297*, 2229–2232.
- (7) Venkatasubramanian, R.; et al. Thin-film thermoelectric devices with high room-temperature figures of merit. *Nature* **2001**, *413*, 507–602.
- (8) Hochbaum, A.; Chen, R.; Diaz Delgado, R.; Liang, W.; Garnett, E. C.; Najarian, M.; Majumdar, A.; Yang, P. Enhanced thermoelectric performance of rough silicon nanowires. *Nature* **2008**, *451*, 163–167.
- (9) Bukai, A.; Bunimovich, Y.; Tahir-Kheli, J.; Yu, J.-K.; Goddard, W. A., III.; Heath, J. R. Silicon nanowires as efficient thermoelectric materials. *Nature* **2008**, *451*, 168–171.
- (10) Wang, R. Y.; Feser, J. P.; Lee, J.-S.; Talapin, D. V.; Segalman, R.; Majumdar, A. Enhanced thermopower in PbSe nanocrystal quantum dot superlattices. *Nano Lett.* **2008**, *8*, 2283–2288.
- (11) Hsu, K. F.; Loo, S.; Guo, F.; Chen, W.; Dyck, J. S.; Uher, C.; Hogan, T.; Polychroniadis, E. K.; Kanatzidis, M. G. Cubic  $\text{AgPb}_m\text{SbTe}_{2+m}$ : Bulk thermoelectric materials with high figure of merit. *Science* **2004**, *303*, 818–821.
- (12) Cho, K.-S.; Talapin, D. V.; Gaschler, W.; Murray, C. B. Designing PbSe nanowires and nanorings through oriented attachment of nanoparticles. *J. Am. Chem. Soc.* **2005**, *127*, 7140–7147.
- (13) Small, J. P.; Perez, K. M.; Kim, P. Modulation of thermoelectric power of individual carbon nanotubes. *Phys. Rev. Lett.* **2003**, *91*, 256801.
- (14) Lianuno, M. C.; Fischer, J. E.; Johnson, A. T., Jr.; Hone, J. Observation of thermopower oscillations in the Coulomb Blockade regime in a semiconducting carbon nanotube. *Nano Lett.* **2004**, *4*, 45–49.
- (15) Groner, M. D.; Fabreguette, F. H.; Elam, J. W.; George, S. M. Low-temperature  $\text{Al}_2\text{O}_3$  atomic layer deposition. *Chem. Mater.* **2004**, *16*, 639–645.
- (16) Talapin, D. V.; Murray, C. B. PbSe nanocrystal solids for n- and p-channel thin film field-effect transistors. *Science* **2005**, *310*, 86–89.
- (17) Zhu, J.; Peng, H.; Chan, C. K.; Jarausch, K.; Zhang, X. F.; Cui, Y. Hyperbranched lead selenide networks. *Nano Lett.* **2007**, *7*, 1095.
- (18) Lin, Y.; Dresselhaus, M. S. Thermoelectric properties of superlattice nanowires. *Phys. Rev. B* **2003**, *68*, 075304.
- (19) Kosmulski, M. In *Encyclopedia of Surface and Colloid Science*; Hubbard, A. T., Ed.; Marcel Dekker: New York; 2002; pp 1627–1636.
- (20) Cui, Y.; Duan, X.; Hu, J.; Lieber, C. M. Doping and electrical transport in silicon nanowires. *J. Phys. Chem. B* **2000**, *104*, 5213–5216.
- (21) Khanal, D. R.; Wu, J. Gate coupling and charge distribution in nanowire field effect transistors. *Nano Lett.* **2007**, *7*, 2778–2783.
- (22) Allgaier, R.; Scanlon, W. Mobility of electrons and holes in PbS, PbSe and PbTe between room temperature and 4.2 K. *Phys. Rev.* **1958**, *111*, 1029–1037.
- (23) Fritzsche, H. A general expression for the thermoelectric power. *Solid State Commun.* **1971**, *9*, 1813–1815.
- (24) Pernstich, K. P.; Rassner, B.; Batlogg, B. Field-effect-modulated Seebeck coefficient in organic semiconductors. *Nat. Mater.* **2008**, *7*, 321–325.
- (25) Brandt, M. S. Thermopower investigation of n- and p-type GaN. *Phys. Rev. B* **1998**, *58*, 7786–7791.
- (26) Li, D.; Wu, Y.; Kim, P.; Shi, L.; Yang, P.; Majumdar, A. Thermal conductivity of individual silicon nanowires. *Appl. Phys. Lett.* **2003**, *83*, 2934–2936.
- (27) Shi, L.; Li, D.; Yu, C.; Jang, W.; Kim, D.; Yao, Z.; Kim, P.; Majumdar, A. Measuring thermal and thermoelectric properties of one-dimensional nanostructures using a microfabricated device. *J. Heat Transfer* **2003**, *125*, 881–888.
- (28) Fardy, M.; Hochbaum, A. I.; Goldberger, J.; Zhang, M. M.; Yang, P. Synthesis and thermoelectrical characterization of lead chalcogenide nanowires. *Adv. Mater.* **2007**, *19*, 3047–3051.
- (29) Gray, D. E. American Institute of Physics Handbook, 3rd ed.; McGraw-Hill: New York, 1972.
- (30) Geig, D. Thermoelectricity and thermal conductivity in the lead sulfide group of semiconductors. *Phys. Rev.* **1960**, *120*, 358.

NL900377E